Approaching the limit of Cu^{II}/Cu^{I} mixed valency in a $Cu^{I}Br_2$/*N*-methylquinoxalinium hybrid compound

Nicolas Leblanc,[a] Stephen Sproules,[c] Claude Pasquier,*[d] Pascale Auban-Senzier,[d] Helene Raffey,[d] and Annie Powell*[a,b]*

[a] Institut für Nanotechnologie, Karlsruher Institut für Technologie , Hermann- von-Helmholtz-Platz 1,D-76344 Eggenstein-Leopoldshafen, Germany.

[b] Institut für Anorganische Chemie, Karlsruher Institut für Technologie, Engesserstra² e 15, D-76131, Karlsruhe, Germany.

[c] University of Glasgow, School of Chemistry, Joseph Black Building A5-14, University Avenue, Glasgow, G12 8QQ, United Kingdom.

[d] Laboratoire de Physique des Solides, UMR-CNRS 8502, Bat. 510, Université Paris Sud, 91405 Orsay Cedex, France.

E-mail: nicolas.leblanc@partner.kit.edu; annie.powell@kit.edu

Abstract. A novel 1D hybrid salt (MQ)[$CuBr_2$]**.** (MQ= *N*-methylquinoxalinium) is reported. Structural, spectroscopic and magnetic investigations reveal a minimal Cu^{II} doping of less than 0.1%. However it is not possible to distinguish Cu^{I} and Cu^{II}. The unusually close packing of the organic moieties and the dark brown colour of the crystals suggest a defect electronic structure.

The chemistry of copper (I) halides has provided an impressive library of compounds, characterized by their structural diversity,[1] In some case, owing to the oxidative instability of the starting material $Cu^{I}X$ (X = Cl, Br, I), pure Cu^{II} or mixed valence Cu^{I}/Cu^{II} can result.[2] In the case of mixed valency, depending on how differentiable the two Cu^{I} and Cu^{II} metal sites are crystallographically, Robin & Day classified them in terms of three different classes. In class I, the sites are fully distinguishable, in class III indistinguishable, and in class II there is an intermediate situation.[3]

In the field of 1D copper bromide based compounds, only a few examples of mixed valency have been reported,[4] and of particular interest is the influence that the amount of Cu^{II} present has on the electronic structure. Here we present a novel 1D copper bromide hybrid compound (MQ)[$CuBr_2$]**.** (MQ = *N*-methylquinoxalinium) which has a tiny amount of Cu^{II} (<0.1%), and yet shows properties consistent with a mixed valent electronic structure.

Colourless crystals of the starting material (MQ)[BF_4] were obtained by recrystallization from MeOH at -20 °C. Crystals of (MQ)[$CuBr_2$]**.** were obtained by the slow vapour diffusion method. Dissolution in warm DMSO of a stoichiometric amount of (MQ)[BF_4] with NaBr and freshly prepared $Cu^{I}Br$ leads to a brown solution after cooling to room

temperature. Upon slow vapour diffusion of MeOH, dark brown crystals formed within a few hours. Phase purity was checked by XRPD (ESI†).

The X-ray crystal structure of (MQ)[$CuBr_2$]**.** was measured at room temperature (293 K) and refined in the space group *C*2/*m*. The structure has infinite 1D [$CuBr_2$]**.** chains composed of edge-sharing [$CuBr_4$] distorted tetrahedra,[4b,5] separated by infinite stacks of *N*-methylquinoxalinium moieties (MQ). These lead to a slightly distorted chessboard packing by virtue of the ² H 97° angle, when viewed along the *b* axis (Fig. 1a). In the inorganic part, the asymmetric unit contains one half copper lying on the 2-fold axis (0, *y*, 0) and two half bromide lying in the mirror plane (*x*, 0, *z*) (Fig. 1b).

The geometry of the coordination sphere is distorted from ideal tetrahedral symmetry (T_d) to give the D_{2d} symmetry, as confirmed by the data from Table S1. The values of the interligand dihedral angles average 80° (from 77.7 to 84.4°) rather than the expected 90° for a perfect T_d symmetry. The values of the edge central and face-edge-face angles significantly differ from the ideal T_d values of 109.5° (from 95° to 117°) and 70.53° (from 60.4° to 78.8°) respectively. Significant changes also occur in the Cu–Br bond lengths and Cu–Br–Cu bridging angles (Cu_1–Br_2 = 2.493 Å, Cu_1–Br_2–Cu_1 = 73.8° and Cu_1–Br_1 = 2.535 Å, Cu_1–Br_1–Cu_1 = 84.7°). This leads to the Cu metal ion being off-centred. This, in turn leads to alternating long-short-long-short Cu–Cu distances of 3.415(1) Å and 2.995(1) Å respectively, and to an increase of the Br_1–Cu_1–Br_2 *trans*-angle to 117.5°.

Regarding the organic part of this hybrid structure, the corresponding bond distances and angles of the MQ moiety are listed in Table S2 (ESI†) and compared with those measured in some related compounds. According to the Cambridge Structural Database only two other salts based on the MQ unit, (MQ)[TCNQ][6] and $(MQ)_2\{H_2\text{-}[Fe^{II}(CN)_6]\}$,[7] have been

reported up to now but only $(MQ)_2\{H_2\text{-}[Fe^{II}(CN)_6]\}$ has been characterized by single crystal X-ray diffraction. Because of such a lack of comparable structures, the simple starting product $(MQ)[BF_4]$ (ESI†) was also characterized by single crystal X-ray diffraction, and its structural data added for comparison. In $(MQ)[CuBr_2]$**.** , the MQ moiety is planar. The quinoxaline core is consistent with an aromatic À-conjugated system with bond distances (C_{sp2}–C_{sp2}, C_{sp2}–N) and planar angles, ranging from 1.30 to 1.41 Å and 117.1 to 123.3°, respectively, which correspond to what has been observed in $(MQ)[BF_4]$, as well as in some other aromatic compounds like naphthalene or pyrazine,[8] but differ significantly from those measured in $(MQ)_2\{H_2\text{-}[Fe^{II}(CN)_6]\}$.[7]

In $(MQ)[CuBr_2]$**.** , one half MQ moiety contributes to the organic part of the asymmetric unit and is located in a mirror plane perpendicular to the *b* axis (*x*,0,*z*). In the (*ac*) plane the MQ molecule interacts with its neighbours (X) only through side contacts via hydrogen bonds ($X\cdots H\text{–}C_{aromatic}$) (Fig. 2, red dashed lines). These occur between either two MQs related by a symmetry centre (0,0,$^1/_2$) (X = N_2, $d_{N2\cdots H8\text{-}C}$ = 2.656 (5) Å, £r_{vdw} (N···H) = 2.75 Å) or between MQ and its surrounding bromide anions (X = Br, $d_{Br22\cdot\cdot H5\text{–}C}$ = 2.962 (1) Å, $d_{Br12\cdot\cdot H9\text{–}C}$ = 3.036 (1) Å, £r_{vdw} (Br…H) = 3.05 Å). Additional hydrogen bonds are present between the methyl group of MQ and the bromide anions either in the (*ac*) plane ($d_{Br1\cdots H1C\text{–}C}$ = 3.054(73) Å) or along the *b* axis ($d_{Br12\cdot\cdot H1B\text{–}C}$ = 2.808 (50) Å) and contribute to the reinforcement of the packing density.

When viewed perpendicular to the *b* axis, the structure of $(MQ)[CuBr_2]$**.** shows an infinite stack of antiparallel displaced[9] MQ molecules related by a symmetry centre ($^1/_4$,$^1/_4$,$^1/_2$ – Fig. 1c and d). The stacking parameters, based on the model of Glówka *et al.*,[10] lead to an effective stacking surface of about 12% and to an interplanar distance *h* =

$^{b}/_{2}$ of 3.205 Å (Fig. S1, ESI†). This distance is surprisingly short compared to the average value, ⟨*h*⟩ = 3.41 Å e £r_{vdw} C···C = 3.40 Å, observed in $(MQ)_2\{H_2\text{-}[Fe^{II}(CN)_6]\}$ and in some similar cationic À-deficient heterocycles like *N*-methylphenazinium (NMP), *N*-methylquinolinium (Q) and *N*-methylacridinium (N-MeA), which stack in a similar way (Table S3).[7,11] Although in a cationic N-rich aromatic heterocycle an interplanar distance of 3.0–3.22 Å (at 173 K) has been reported,[12] this distance we observe in $(MQ)[CuBr_2]$**.** is by far the shortest interplanar distance reported for cationic À-deficient heterocycles. Such a distance with $d < 3.30$ Å is usually observed in strongly interacting cation radical or mixed-valence salts.[13] This raised the question concerning the charge distribution within the $(MQ)[CuBr_2]$**.** salt, and especially the respective oxidation states of all moieties.

In terms of the synthesis, crystals of $(MQ)[CuBr_2]$**.** were obtained by heating a solution of $Cu^{I}Br$ under aerobic conditions, which tends to destabilize Cu^{I} to Cu^{II} (ESI†). This is reinforced by the electron acceptor behaviour of the *N*-methylquinoxalinium cation, which can be irreversibly reduced in solution as a neutral radical (E = -0.87 V *vs*. Fc/Fc^{+} – Fig. S2, ESI†). For these reasons, it is reasonable to suggest that both Cu^{II}/Cu^{I} and $MQ^{I}/MQ^{Ï}$ species could be stabilised in the crystalline state.

The single crystal X-ray structure analysis of $(MQ)[CuBr_2]$**.** show features that are consistent with the presence of Cu^{I} and MQ^{I} in the crystal. In the inorganic part, the distorted tetrahedral environment around the copper is in line with a four-coordinated Cu^{I},[4e,14] while Cu^{II} would prefer a square planar geometry.[5c,15] In the specific case of mixed valent compounds having the same coordination environment,[4a-d] the Cu–Br bond distances criterion dominates. Here the average Cu–Br distance of 2.51 Å is consistent

with the one found in similar pure $Cu^{I}Br$ based salts (2.506 Å),[4e,14] whereas the comparable $Cu^{II}Br$ bond length is shorter with an average value of 2.422 Å.[5c,15] In the organic part, the structure, IR vibrations (Fig. S3, ESI†) and the redox state of MQ in (MQ)[$CuBr_2$]**.** are similar to (MQ)[BF_4] (Table S2, ESI†), where the cationic state MQ^{I} is clear. Thus, according to the X-ray structure analysis, we have a pure (MQ^{I})[$Cu^{I}Br_2$]**.** composition.

The X-band EPR spectrum of (MQ)[$CuBr_2$]**.** shows a broad signal with g ~ 2.042 (Fig. S4, ESI†). This g-value is higher than typical for organic-based radical spins and thus reveals the presence of Cu^{II} in the polycrystalline material. The fluid solution spectrum in DMSO was recorded at 333 K to improve the motional tumbling in this viscous solvent. The complicated sequence of peaks appears to arise from three difference Cu^{II} species; only two four-line patterns can be clearly identified (Fig. S5, ESI†). There was no evidence of an organic-based radical signal attributable to $MQ^{Ï}$ or to $Br^{Ï}$ in the spectrum. This signal is consistent with less than 0.4% of the copper ions in the sample based on spin counting. There is insufficient resolution to decipher the chemical environment of the copper. Exposure to the atmosphere sees the growth of a prominent of a signal at g ~ 2.17 that perfectly matches the profile of $CuBr_2$ dissolved in DMSO solution (Fig. S6, ESI†).

A Bond Valence Sum (BVS) treatment [equation $V_{Cu} = 2 \times S_{Cu–Br1} + 2 \times S_{Cu–Br2}$; $S = \exp(R_0 - R)/B$], using the most recent bond valence parameter table,[16] leads to the oxidation state V_{Cu} = +1.083, which is in line with the suggestion that the copper in this compound is nearly exclusively Cu^{I}.

The magnetic susceptibility of (MQ)[$CuBr_2$]**.** was measured on a polycrystalline sample (223 mg) from 4.5–300 K under an applied field of 0.4 and 1 T. As shown in Fig. 3a, the

susceptibility is negative which confirms the dominant diamagnetic nature of the compound. The fitted molar diamagnetic susceptibilities at 0.4 and 1 T gives an average value χ_M = -173.26 × 10^{-6} emu mol^{-1}, which is in line with the approximation χ_M = $M_{(MQ)[CuBr]2}$. = 368.54/2 = 184.27 × 10^{-6} emu mol^{-1} and with the one calculated from the Pascal's Constants[17] (χ_M = -140.12 × 10^{-6} emu mol^{-1}).

In order to determine the amount of Cu^{II} present in the compound a global fitting of the difference plots of $\chi - \chi_{dia}$ (T) (*H* = 0.4 and 1T) is typical of a paramagnetic species which follows a Curie-Weiss law with weak antiferromagnetic interactions (C = 212.766 10^{-6} emu K mol^{-1}, ¸ = -2.404 K – Fig. 3b + inset). Extraction of the Curie constant gives an estimation of about 0.054% of Cu^{II} present in the compound, when comparing the Curie constant of a corresponding pure Cu^{II} paramagnet (C = 0.391 emu K mol^{-1} with $S = {}^1/_2$, g_{eff} = 2.042). Thus according to the X-ray, EPR, BVS, and SQUID measurements, the amount of Cu^{II} within the compound is clearly negligible, and could be explained as arising from some defects at the surface of the crystals, which is a well-known phenomenon in the chemistry of Cu^{I}.

However this is not consistent with the homogenous dark brown colour of the crystals (Fig. 4) which persists even upon grinding. Furthermore, the electronic spectrum of (MQ)[$CuBr_2$]**.** reveals two broad absorption bands, one in the UV-Visible region (200–800 nm), and the other in the near-infrared (600–1200 nm, λ_{max} H 900 nm). This colour cannot arise from the MQ^{I} cation which displays a unique À-À* transition in the UV region (λ_{max} = 335 nm, Fig. 4). Similarly a pure copper(I) bromide species should also give colourless crystals due to the d^{10} electronic configuration of Cu^{I} and the impossibility of ligand to metal charge transfer.[5a,18] An electronic transition arising from a charge

transfer between the electron donors (Cu^{I} or Br^{-}) and the acceptor MQ^{I}, as originally postulated in the study of some paraquat (MV^{2+}) salts[4c,19] is not possible. In the MV^{2+} salts the authors attribute the colour of the crystals to the presence of some Cu^{II} sites and $MV^{\ddot{I}+}$ cation radicals in the solid, resulting from a halide-mediated electron transfer between the Cu^{I} and MV^{2+}. This is only possible when the orbitals of the halide (X) interact suitably with those of the pyridinium site (N^{+}) of the electron acceptor, which is characterized by a short $X\cdots N^{+}$ contact and an almost perpendicular angle between the halide and the pyridinium plane.[4c,20] In $(MQ)[CuBr_2]$**.** , in addition to the fact that there is no evidence of any $MQ^{\ddot{I}}$ from the EPR measurements, such a donor-acceptor interaction is not present, since the bromide anions are 37° shifted from the ideal 90° for a "$Br\cdots N^{+}$" geometry, and the shortest distance ($Br_22\cdot\cdot N_1$) is much longer than the sum of the Van der Waals radii [$d_{Br22\cdot\cdot N1}$ = 4.024(2) Å; £r_{vdw} (Br···N) = 3.4 Å; Fig. 2, blue dashed line]. This leads to the conclusion that a pure $MQ^{I}/Cu^{I}/Br^{-}$ composition should give colourless crystals of $(MQ)[CuBr_2]$**.** .

In the case of Cu^{I}/Cu^{II} mixed valence the d^9 configuration of Cu^{II} can explain the colours of the compounds.[4a-d] The absorption bands usually arise from Cu^{II} metal centred transitions and from ligand-to-metal charge transfer (LMCT) bands, while an additional transition at lower energy can be attributed to an intervalence charge transfer band (IVCT).[4b] However, dark colours such as green or deep blue are explained when the amount of Cu^{II} is significant in the solid (e 50%).[4a,b] In the case of $(pq)[Cu_2Br_4]$,[4c] which has only 2% Cu^{II}, the reddish-orange colour arises from charge transfer. In our case, with less than 0.1% Cu^{II} and because no charge transfer can occur, we need to find a different explanation for the dark brown colour with such a long absorption range (400–1200 nm).

Our first interpretation of the results postulated itinerant electrons mediated by the crystal packing. Single crystal conductivity measurements were carried out along the *b* axis, since this corresponds to the [$CuBr_2$]**.** chain and to the À-stacking axis of the MQ moieties directions and is expected to be the preferential conduction path. The temperature dependence of the conductivity shows an activated behavior, and the conductivity at room temperature is estimated as 3×10^{-9} S m^{-1} (Fig. S7, ESI†). The fit of the data to an Arrhenius law with $\tilde{A} = \tilde{A}_0 \exp(-E_a/T)$ gives an activation energy E_a of 7500 K *i.e.* an energy gap of ” = $2E_a$ = 1.3 eV a little higher than the optical gap.

This value of conductivity is about 300 times smaller than the one reported in (pq)[Cu_2Br_4],[4c] containing 2% Cu^{II} and acting as mediator of the charge transport. This actually in line with the conductivity value we find giving an estimate of about 0.01% Cu^{II}, acting as a charge carrier in our compound. As in the case of Scott & Willet[4c] we conclude that the observed properties are intrinsic to the system and not due to surface effects.

The authors thank the financial support provided by the Alexander von Humboldt Foundation (fellowship to N.L.) and Helmholtz POF “STN”. We also thank Dr. Lionel Sanguinet for the electrochemistry measurements.

Notes and references

† Electronic supplementary information (ESI) available: Tables of crystal and X-Ray crystallographic files in CIF format, XRPD patterns, UV-Vis and IR spectra of (MQ)[$CuBr_2$]**.** and (MQ)[BF_4], the additional EPR spectra of (MQ)[$CuBr_2$]**.** , and cyclic

voltammogram of (MQ)[BF_4]. CCDC 1400365 and 1400362. For ESI and crystallographic data in CIF or other electronic format see DOI: 10.1039/x0xx00000x

‡ Crystal data of (MQ)[$CuBr_2$]**.** : $C_9H_9N_2Cu_1Br_2$, M = 368.354; monoclinic, $C2/m$; a = 15.373(2) Å, b = 6.4099(7) Å, c = 10.9646(18) Å, ² = 96.692(12)°, V=1073.1(3) $Å^3$; Z = 4; T = 293K; $R_1(F)$ = 0.029 [1265 unique reflections in the 3.4–27.3° ¸ range (R_{int} = 0.022), of which 1133 had $I > 2\tilde{A}(I)$, 92 parameters refined], $wR_2(F_2)$ = 0.091 (all data), GOF = 1.32; max/min residual electron density 0.390/–0.582 e $Å^{-3}$. Single crystals X-Ray diffraction data of (MQ)[$CuBr_2$]**.** and (MQ)[BF_4] were collected at 293K on a STOE IPDS II Diffractometer equipped with a graphite monochromatized Mo K± radiation (» = 0.71073 Å). Structures were solved and refined using the WinGX2013 package[21] and molecular diagrams were prepared using Diamond 3.2i.[22] Positions, atomic displacement parameters were refined by full-matrix least-squares routines against F^2, including hydrogens atoms of the methyl group. Hydrogen atoms of the pyrazinium moiety were placed at calculated positions and refined using a riding model.

1. R. Peng, M. Li and D. Li, *Coord. Chem. Rev.*, 2010, **254**, 1-18.
2. (a) H. Feng, X.-P. Zhou, T. Wu, D. Li, Y.-G. Yin and S. W. Ng, *Inorg. Chim. Acta*, 2006, **359**, 4027-4035; (b) Y. Cui, Y. Yue, G. Qian and B. Chen, *Chem. Rev.*, 2011, **112**, 1126-1162.
3. (a) M. Robin and P. Day, in *Advances in Inorganic Chemistry Volume 10*, Elsevier, 1968, vol. 10, pp. 247-422; (b) P. Day, N. S. Hush and R. J. H. Clark, *Phil. Trans. Roy. Soc. A*, 2008, **366**, 5-14.

4. (a) R. D. Willett, *Inorg. Chem.*, 1987, **26**, 3423-3424; (b) B. Scott, R. Willett, L. Porter and J. Williams, *Inorg. Chem.*, 1992, **31**, 2483-2492; (c) B. Scott, R. Willett, A. Saccani, F. Sandrolini and B. L. Ramakrishna, *Inorg. Chim. Acta*, 1996, **248**, 73-80; (d) G. Margraf, M. Bolte, M. Wagner and H.-W. Lerner, *J. Chem. Crystallogr.*, 2007, **37**, 503-506; (e) M. Stricker, T. Linder, B. Oelkers and J. Sundermeyer, *Green Chem.*, 2010, **12**, 1589-1598.

5. (a) R. D. Willett and B. Twamley, *Inorg. Chem.*, 2004, **43**, 954-957; (b) J. Sertucha, A. Luque, F. Lloret and P. Román, *Polyhedron*, 1999, **17**, 3875-3880; (c) R. Fletcher, J. J. Hansen, J. Livermore and R. D. Willett, *Inorg. Chem.*, 1983, **22**, 330-334.

6. H. J. Keller, D. Noethe and M. Werner, *Can. J. Chem.*, 1979, **57**, 1033-1036.

7. S. I. Gorelsky, A. B. Ilyukhin, P. V. Kholin, V. Y. Kotov, B. V. Lokshin and N. V. Sapoletova, *Inorg. Chim. Acta*, 2007, **360**, 2573-2582.

8. F. H. Allen, O. Kennard, D. G. Watson, L. Brammer, A. G. Orpen and R. Taylor, *J. Chem. Soc., Perkin Trans. 2*, 1987, S1-S19.

9. N. Hayashi, H. Higuchi and K. Ninomiya, in *Heterocyclic Supramolecules II*, eds. K. MatsumotoN. Hayashi, Springer Berlin Heidelberg, 2009, vol. 18, pp. 103-118.

10. M. L. Główka, D. Martynowski and K. Kozłowska, *J. Mol. Struct.*, 1999, **474**, 81-89.

11. (a) S. Kim, H. Namgung and H. M. Lee, *J. Kor. Chem. Soc.*, 1994, **38**, 827-832; (b) P. Kuppusamy, B. L. Ramakrishna and P. T. Manoharan, *Inorg. Chem.*, 1984, **23**, 3886-3892; (c) H. Namgung, S.-B. Kim and I.-H. Suh, *Acta Cryst. C*, 1998, **54**, 612-614; (d) C. Mahadevan, M. Seshasayee, P. Kuppusamy and P. T. Manoharan, *J. Cryst. Spectrosc .*, 1985, **15**, 305-316; (e) C. J. Fritchie, *Act. Cryst.*, 1966, **20**, 892-898; (f) P. Kuppusamy, P. T. Manoharan, C. Mahadevan and M. Seshasayee, *J. Cryst.*

Spectrosc., 1985, **15**, 359-376; (g) K. Ueda, T. Sugimoto and T. Mochida, *Acta Cryst. E*, 2001, **57**, o578-o580; (h) H. Endres, H. J. Keller, W. Moroni and D. Nothe, *Acta Cryst. B*, 1979, **35**, 353-357; (i) J. Y. Niu, J. P. Wang and Z. Y. Zhou, *Chin. J. Inorg. Chem.*, 2000, 647-652; (j) J. P. Wang, J. Y. Niu, D. B. Dang and Y. Bo, *Chin. J. App. Chem.*, 2002, 144-148; (k) T. M. Bockman and J. K. Kochi, *J. Am. Chem. Soc.*, 1989, **111**, 4669-4683; (l) L. F. Yang, Z. H. Peng, G. Z. Cheng and S. M. Peng, *Polyhedron*, 2003, **22**, 3547-3553; (m) P. Storoniak, K. Krzyminski, P. Dokurno, A. Konitz and J. Blazejowski, *Aust. J. Chem.*, 2000, **53**, 627-633.

12. R. Centore, M. Causà, S. Fusco and A. Carella, *Cryst. Growth Des.*, 2013, **13**, 3255-3260.
13. N. Leblanc, N. Mercier, O. Toma, A. H. Kassiba, L. Zorina, P. Auban-Senzier and C. Pasquier, *Chem. Commun.*, 2013, **49**, 10272-10274.
14. (a) J. P. Lang, H. Z. Zhu, X. Q. Xin and M. Q. Chen, *Chem. J. Chin. U.*, 1992, **13**, 18-21; (b) H. Zhao, Z.-R. Qu, Q. Ye, B. F. Abrahams, Y.-P. Wang, Z.-G. Liu, Z. Xue, R.-G. Xiong and X.-Z. You, *Chem. Mater.*, 2003, **15**, 4166-4168; (c) J.-J. Hou, C.-H. Guo and X.-M. Zhang, *Inorg. Chim. Acta*, 2006, **359**, 3991-3995; (d) G. Noshtchenko, V. Kinzhybalo, T. Lis and B. Mykhalitchko, *Z. Anorg. Allg. Chem.*, 2007, **633**, 306-309.
15. (a) U. Geiser, R. D. Willett, M. Lindbeck and K. Emerson, *J. Am. Chem. Soc.*, 1986, **108**, 1173-1179; (b) T. E. Grigereit, B. L. Ramakrishna, H. Place, R. D. Willett, G. C. Pellacani, T. Manfredini, L. Menabue, A. Bonomartini-Corradi and L. P. Battaglia, *Inorg. Chem.*, 1987, **26**, 2235-2243; (c) K. Murray and R. D. Willett, *Acta Cryst. C*, 1991, **47**, 2660-2662; (d) M. R. Bond, H. Place, Z. Wang, R. D. Willett, Y. Liu, T. E.

Grigereit, J. E. Drumheller and G. F. Tuthill, *Inorg. Chem.*, 1995, **34**, 3134-3141; (e) S. Lorenzo, C. Horn, D. Craig, M. Scudder and I. Dance, *Inorg. Chem.*, 2000, **39**, 401-405; (f) S. Haddad, F. Awwadi and R. D. Willett, *Cryst. Growth Des.*, 2003, **3**, 501-505; (g) A. Kelley, S. Akkina, G. K. Devarapally, S. Nalla, D. Pasam, S. Madhabushi and M. R. Bond, *Acta Cryst. C*, 2011, **67**, m22-m34.

16. (a) I. D. Brown and D. Altermatt, *Acta Cryst. B*, 1985, **41**, 244-247; (b) *"Bond Valence Parameters"*, IUCr., 2013.
17. (a) G. A. Bain and J. F. Berry, *J. Chem. Edu.*, 2008, **85**, 532; (b) C. J. O'Connor, P*rog. Inorg. Chem.*, John Wiley & Sons, Inc., 2007, pp. 203-283.
18. N. Armaroli, G. Accorsi, F. Cardinali and A. Listorti, in *Photochemistry and Photophysics of Coordination Compounds I*, eds. V. BalzaniS. Campagna, Springer Berlin Heidelberg, 2007, vol. 280, pp. 69-115.
19. A. J. Macfarlane and R. J. P. Williams, *J. Chem. Soc. A.*, 1969, 1517-1520.
20. N. Leblanc, M. Allain, N. Mercier and L. Sanguinet, *Cryst. Growth Des.*, 2011, **11**, 2064-2069.
21. L. Farrugia, *J. Appl. Cryst.*, 2012, **45**, 849-854.
22. H. Putz and K. Brandenburg, *Diamond - Crystal and Molecular Structure Visualization, Kreuzherrenstr. 102, 53227 Bonn, Germany*.

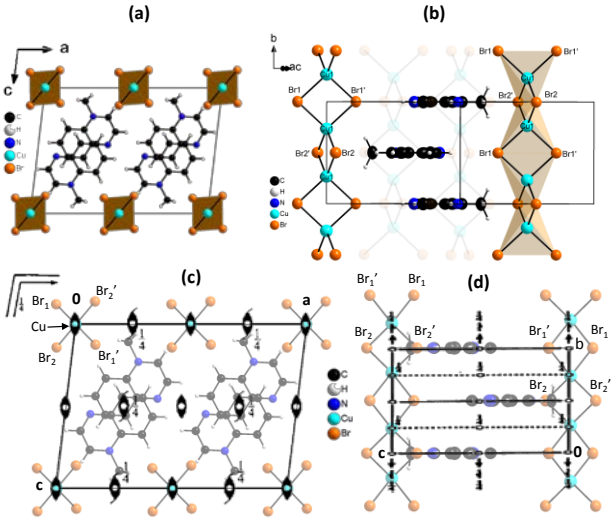

Fig. 1 (a) General view of (MQ)[$CuBr_2$]**.** along the *b* axis. (b) - Partial view perpendicular to the direction (20–1). The close packing within the organic network and the two [$CuBr_2$]**.** chains related by the C-centred Bravais lattice are displayed. (c, d) Overlaid view with the projected symmetry elements of the *C*2/*m* space group, along the *b* axis (c) and the *a* axis (d).

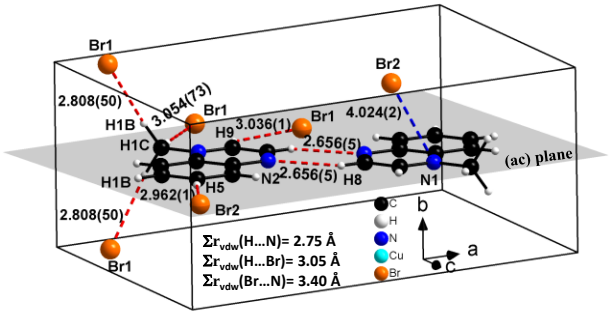

Fig. 2 Partial view of (MQ)[$CuBr_2$]**.** showing the hydrogen bonds (red dashed lines) and the Br–N distance (blue dashed line) between either two MQ or MQ and Br moieties.

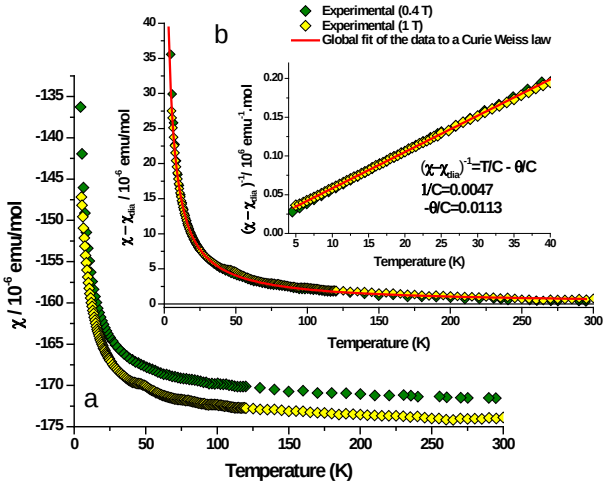

Fig. 3 (a) Plot of the experimental Molar susceptibility versus Temperature of (MQ)[$CuBr_2$]**.** (223 mg, 0.4 and 1T). (b + inset) Plot after diamagnetic correction. The molar paramagnetic susceptibility fits better with a Curie-Weiss law, represented by the red line (global fit parameters: C = 212.766 × 10^{-6} emu K mol^{-1}, ¸ = -2.404 K with $Ç_{dia}$ (0.4 T) = -171.85 × 10^{-6} emu mol^{-1}, $Ç_{dia}$(1T) = -174.68 × 10^{-6} emu mol^{-1}).

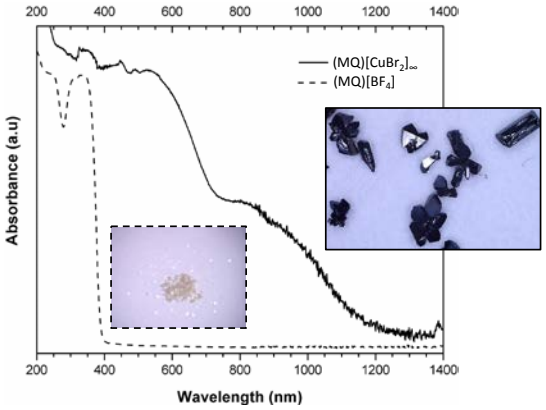

Fig. 4 Solid state UV-Vis-NIR spectra of (MQ)[$CuBr_2$]**.** (solid line) and (MQ)[BF_4] (dashed line) with their corresponding crystals pictures.